

## Flesh Tone Correction Algorithm for TV Receivers

Ionut Mirel

**Abstract** – In this paper, we propose a Flesh Tone Colour Correction Algorithm for broadcast video receivers. Flesh tone regions are a critical processing topic since skin tones are generally the most common to reference. The flesh tone correction region is extracted from the digital colour-difference signals (B-Y, R-Y) and adjusted for optimal flesh tone display. The correction is applied as colour variation, hence the processing is less intrusive than a full range correction approach and also allows for a cost-effective hardware implementation.

**Keywords:** Flesh Tone Correction, flesh toning, YUV, RGB, IQ, NTSC, PAL

### I. INTRODUCTION

Very complex Flesh Tone Correction (FTC) methods are used in pattern and face recognition applications [1, 2, 3, 4, 5, 6]. However, in consumers applications where cost vrs. quality are the reigning requirements these methods find little application. The present algorithm although very low-cost allows for high quality FTC processing.

### II. GENERAL CONSIDERATIONS

Flesh tones are located close to a  $123^\circ$  rotated +U axis in the  $[U, V]$  color space having a hue range slightly off by  $+15^\circ$  toward Red and  $-15^\circ$  toward Yellow. The saturation range is from 25% to 75%; therefore mainly saturation and not hue is the major to accurate flesh tone reproduction.

The Flesh Tone Region processing can be more conveniently performed in a rotated by  $33^\circ$  version of the  $UV$  color space. In literature [7] the rotated  $UV$  space is referred to as the  $IQ$  space. The rotated U axis is called "I" axis. Similar to the V axis - a corresponding "Q" axis, in quadrature with the "I" axis is defined. For convenience the  $[I, Q]$  space is symmetrical around the zero level point, by shifting the  $[U, V]$  space by 112 levels for 8 bit signal levels.

A typical flesh tone correction circuit is searching for colors in the flesh tone area comprised by  $(\pm 7^\circ \pm 30^\circ)$  around the +I axis. All colors within this area are corrected to a color closer to the flesh tone. Fig. 1 shows a detailed diagram of the Flesh Tone Region (FTR) in the  $UV$ , resp.  $IQ$  color space [7].

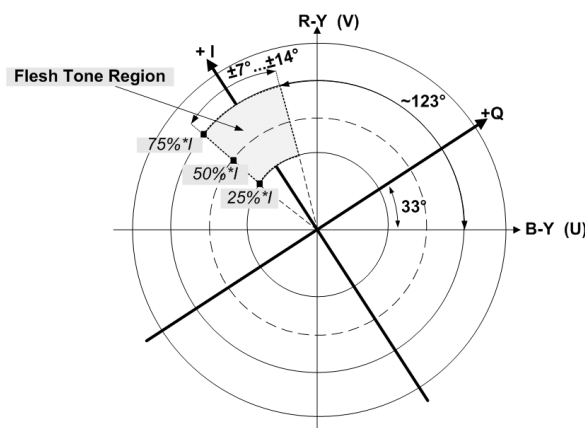


Fig. 1. Flesh Tone Region representation in the UV/IQ Color Space

#### II.1. FLESH TONE CORRECTION METHODS

**II.1.1. Overall  $Q/2$  Correction** - A simple FTC approach may halve all the hue (Q) values. Although very simple, the method corrects also non-flesh tone colors, hence the correction is very image specific.[8]

**II.1.2.  $Q/2$  Correction on Saturation Levels** - A slightly more complex approach is halving the Q values for all colors values between 25% and 75% of the saturation within a  $\pm 30^\circ$  range of the +I axis. The method is mostly suited for analog implementations. [8-10] The method does not provide a non-linear hue correction and thus generates large hue jumps, leading to non-natural corrected flesh tones [11]. The digital implementation of the method is slightly more expensive since it requires a divider for the Flesh Tone angle range calculation[7].

**II.1.3. Flesh Tone Region Detect and Hue Correction** The Flesh Tone Region is extracted from the entire  $[U, V]$  digital color-difference space, as a signal corresponding to the tangent between the two color-difference signals. The Flesh Tone Correction is produced by suitably multiplying the sine and cosine values by the  $[U, V]$  signals. [12, 13] [11] Although it produces good processing quality, the method is correcting the entire  $[I, Q]$  space, thus introducing quantization errors in the entire color space. Compared to other methods, it is more expensive since it uses dividers and large LUT structures. Fig. 2. shows the correction curve proposed in [14]

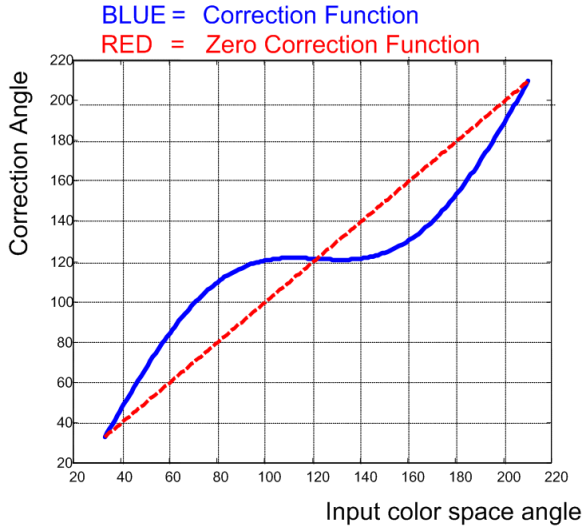


Fig. 2. Possible Correction Curve in the full YUV space

### III. PROPOSED FTC ALGORITHM

#### III.1 Unique Interpolation Curve

The method improves the algorithm in [14] such that the correction is solely performed in the region of interest. Quantization errors are limited to the Flesh Tone Region itself and are also reduced as the correction is applied as color variation. This approach is less intrusive as a full color range correction approach, hence it allows for higher quality correction together with a more efficient implementation.

The initial correction curve can be remapped to its translated versions along the  $I$  axis by simple pixel remapping. This allows for multiple correction curves along the region of interest.

The  $[U, V]$  color space is converted into a  $[I, Q]$  space by simple matrix multiplication.

$$|IQ| = |UV| \cdot \begin{vmatrix} -\sin(\alpha) & \cos(\alpha) \\ \cos(\alpha) & \sin(\alpha) \end{vmatrix} \quad (1)$$

$\alpha$  represents the  $UV$  color space rotation angle. Depending on the geographical region  $\alpha$  can take various values. For Caucasian flesh tones  $\alpha$  is typically  $33^\circ$

In order to produce a smooth correction especially along the FTR boundaries the correction function suggested is of the form

$$y = x + a \cdot \sin(x). \quad (2)$$

The FTC problem can be viewed as a pixel mapping procedure which furthermore can be reduced to a simple geometrical approach as described in Fig. 3. The original  $[U, V]$  coordinate system is rotated by the angular shift ( $\theta=33^\circ$ ) hence generating the  $[I, Q]$  space.

$$\begin{aligned} \theta &\in [33^\circ, 180^\circ + 33^\circ], \\ \Delta\theta &\in [123^\circ - 15^\circ, 123^\circ + 15^\circ] \end{aligned} \quad (3)$$

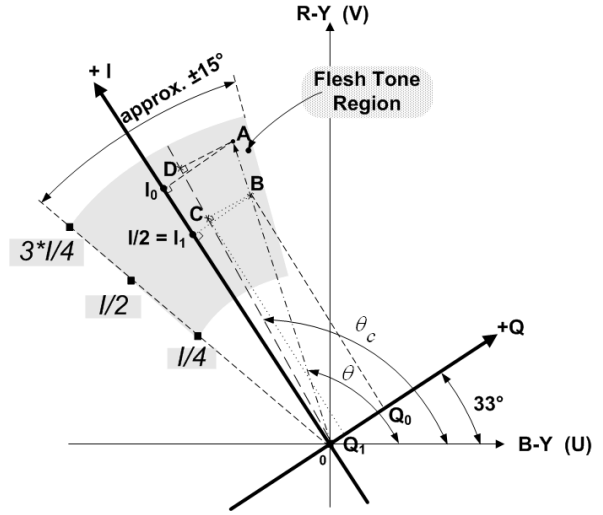


Fig. 3. FTR – Parameters Definition

Applying the sinusoidal correction curve in the new  $[I, Q]$  coordinates, (2) becomes:

$$\theta_c = \Delta\theta + A \cdot \sin\left(2\pi \cdot \frac{\Delta\theta - \min(\Delta\theta)}{2\Delta\theta}\right), \quad (4)$$

The FTR is extracted by calculating the tangent of the rotated flesh tone angle (Fig. 2.):

$$\tan(123^\circ - \theta) = \frac{I_0}{Q_0}, \text{ resp. } \tan(123^\circ - \theta_c) = \frac{I_1}{Q_1} \quad (5)$$

ITU-601 specifies 256 gray levels for the RGB color space. Therefore for  $Y$ ,  $Cr$  and  $Cb$  ranges are mapped in the interval  $(16 \div 240)$ . Therefore  $I_{Max} = 112$ .

$$\theta = \arctan\left(123^\circ - \frac{56}{Q}\right) \quad (6)$$

and from (4) we obtain:

$$\begin{aligned} Q_1 &= \frac{I_{Max}}{2 \cdot \tan(123^\circ - \theta)} = \\ &= \frac{56}{\tan(\Delta\theta) + A \cdot \sin\left(2\pi \cdot \frac{\Delta\theta - \min(\Delta\theta)}{2\Delta\theta}\right)} \end{aligned} \quad (7)$$

For a Flesh-tone aperture of approx.  $\pm 15^\circ$  we can well enough approximate the  $\langle AOD \rangle$  angle with  $\langle AOI \rangle$ . Therefore the following mapping scheme can be used:

$$\begin{aligned} [U, V] &\rightarrow [I, Q_0] \rightarrow \\ &\rightarrow \left[\frac{I}{2}, Q_0\right] \rightarrow \left[\frac{I}{2}, Q_1\right] \rightarrow \\ &\rightarrow [I, Q_1] \rightarrow [U', V'] \end{aligned} \quad (9)$$

This translates into the following point mapping scheme:

$$\mathbf{A} \rightarrow \mathbf{A} \rightarrow \mathbf{B} \rightarrow \mathbf{C} \rightarrow \mathbf{D} \rightarrow \mathbf{D} \quad (10)$$

We could now generate a set of point mappings (i.e.  $Q$  value mappings) for several  $I$  values. However this approach is inefficient, as it requires multiple correction curves.

Therefore to further reduce the implementation, it is assumed that for small angles a single correction curve could be used. The curve would optimize the mapping at  $I/2$ . The unique correction curve was chosen in the middle of the FTR. Hence the relative approximation error is symmetric and very small. Therefore the resulting quality degradation is minimal. The graph of the proposed angular correction function (in " $\theta$ ") is shown in Fig. 4.

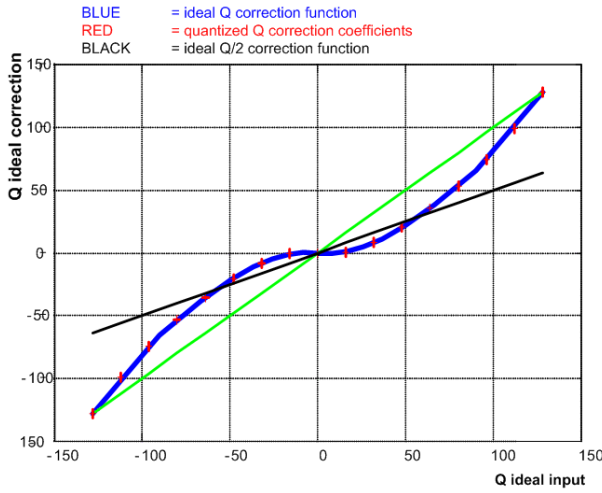


Fig. 4. Proposed Full-Range FTC Transfer Function

The FTC is produced by suitably interpolating the current  $Q$  values by  $Q_{corr}$  values provided through programmable coefficients. Good simulation results have been obtained by using 17 coefficients. Furthermore, since the correction characteristic is symmetric the number of correction coefficients can be folded. Since for  $123^\circ$  the correction is null, the central coefficient will always be zero, thus there is no need of storing it. The method avoids large LUT and dividers. Since the correction is still applied on the entire dynamic range inside the FTR, the method still introduces quantization errors during conversion of  $[U, V]$  into  $[I, Q]$  and back into  $[U, V]$  space. The other source of errors is that it assumes a constant  $I$ , which in reality is not the case.

### III.2 Multiple Interpolation Curves

The corrections for points not on the  $I/2$  axis can be approximated by weighting the correction curve with the corresponding  $I$  value. The interpolated and corrected  $Q$  values are obtained by mapping the current  $Q$  value on the proposed (2).interpolation curve:

$$Q_{corr\_interp} = Q_{corr} \cdot \lambda_{corr} + Q \cdot (1 - \lambda_{corr}) \quad (11)$$

The FTC detection is now reduced to an edge detection along a line characterized by

$$\tan(90 - \theta) = \frac{I_{Max}}{Q_{Max}} \quad (12)$$

For  $\theta = 30^\circ$  all points in the Flesh Tone Region are characterized by  $\tan(90-\theta) = \sqrt{3}$  and  $I \geq Q\sqrt{3}$ .

The other conditions are

$$I \in \left[ \frac{112}{4}, \frac{3 \cdot 112}{4} \right] = [28, 84] \quad (13)$$

and

$$Q \in [-coeff[0], +coeff[0]]$$

to ensure that all corrected  $Q$  values are in the correction range.

### III.3 Variational Approach

The proposed algorithm uses full-range correction coefficients to produce full-range corrected  $Q$  values. This implies need of larger arithmetic circuits. In order to minimize the hardware, but also to maintain the correction quality,  $\Delta Q_{corr}$  values for the correction coefficients can be used. Thus the arithmetic circuits will process only the correction values, and will no longer contain the "base"  $Q$  values which are not changing during the correction process and would only act as offsets on the "to-be-corrected" values. Quantisation errors are limited to the hue-difference values inside the flesh tone region itself, since the correction is solely performed in the region of interest and only on hue-difference values; the signal outside the FTR is bypassed.

The graph of the  $\Delta Q_{corr}$  correction function is shown in Fig. 6. The Blue plot shows the behaviour of the simplest correction using a fixed  $\frac{Q}{2}$  correction.

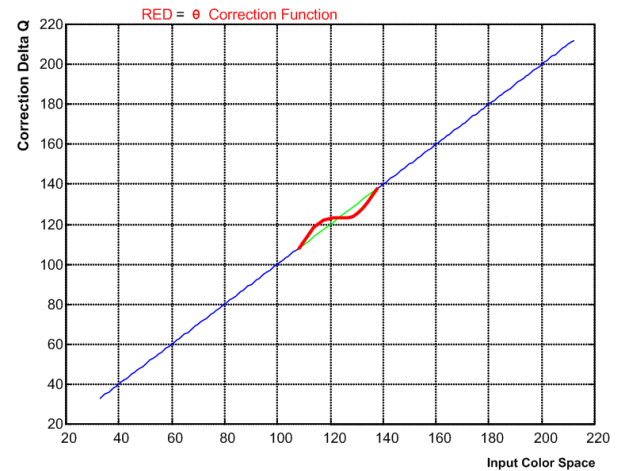


Fig. 5. Proposed FTC Transfer Function on the entire FTR

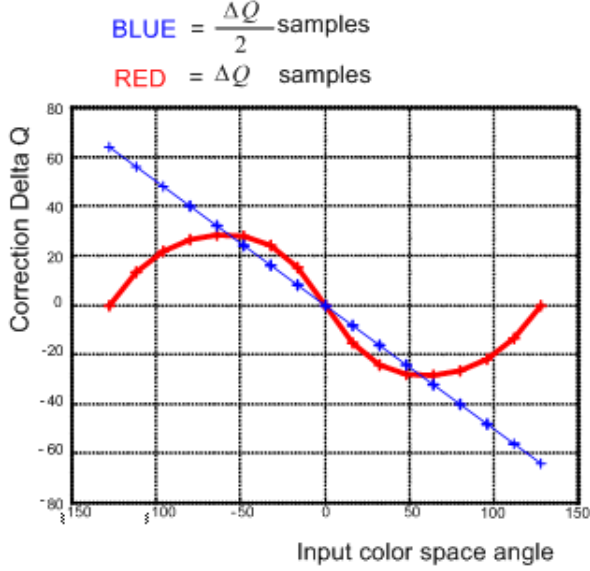


Fig. 6. Detailed - Proposed FTC Transfer Function for whole FTR

The variation range of the  $[I, Q]$  components is the same as the variation range of the  $[U, V]$  components, i.e.  $(16 \div 240)$ .

The graph of the proposed angular correction function (in "0") is shown in Fig. 6. As opposed to correcting for the full range  $Q$  values, the FTC is produced by suitably interpolating the current  $\Delta Q_{corr}$  values.

Assuming  $I = \text{constant}$  and differentiating on  $Q$  :

$$\begin{aligned} \Delta I &= 0 \\ \Delta U &= \Delta Q \cdot \cos(\alpha) \\ \Delta V &= \Delta Q \cdot \sin(\alpha) \end{aligned} \quad (14)$$

Hence the corrected  $[U, V]$  values can be obtained by adding to the current  $[U, V]$  the  $[\Delta U, \Delta V]$  components. Since  $I = \text{constant}$  only the  $\Delta Q$  components are required for the  $[\Delta U, \Delta V]$  calculation. A Similar interpolation curve as above is proposed. To reduce the hardware even further a correction curve for  $I=64$  instead of  $I=52$  is used.

The Region Detection becomes now a simple shift operation hence Eq. 5 becomes:

$$\tan(90 - \theta) = \frac{I_{Max}}{Q_{Max}} = \frac{64}{Q_{Max}} \quad (15)$$

Furthermore, instead of using angular values for the Flesh Tone Region selection, the user can select  $Q$  values as powers of 2 (i.e.  $Q=2,4,8,16,32,64,128,\text{etc.}$ ). Thus (15) becomes:

$$\tan(90 - \theta) = \frac{64}{Q_{Max}} = \frac{64}{2^n}, n \in \mathbb{N} \quad (16).$$

The Block Diagram of the algorithm implementation is presented in Fig. 7.

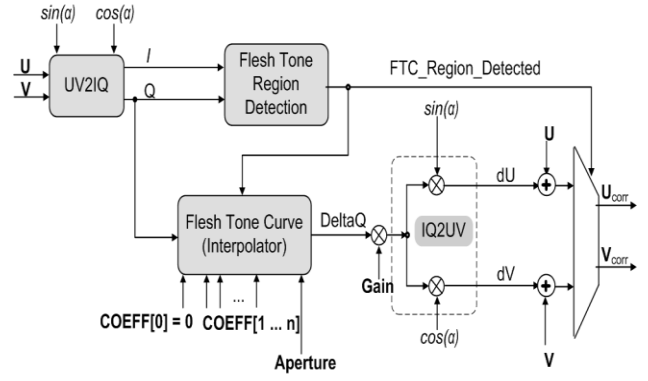
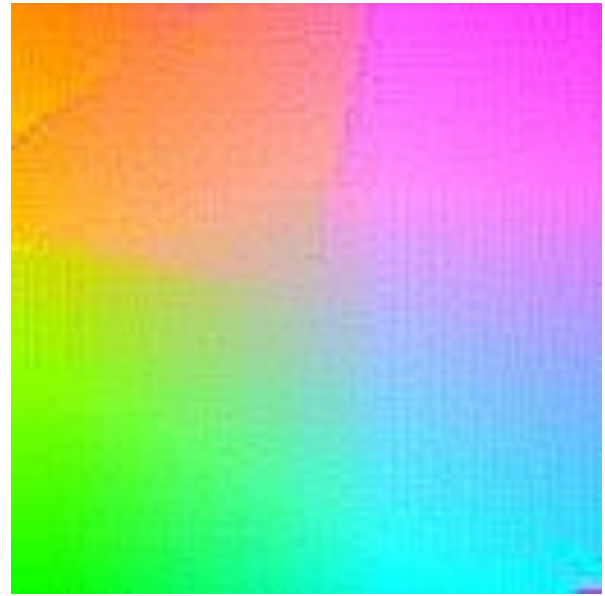


Fig. 7. FTC Block Diagram

#### IV. EXPERIMENTAL RESULTS



(a)

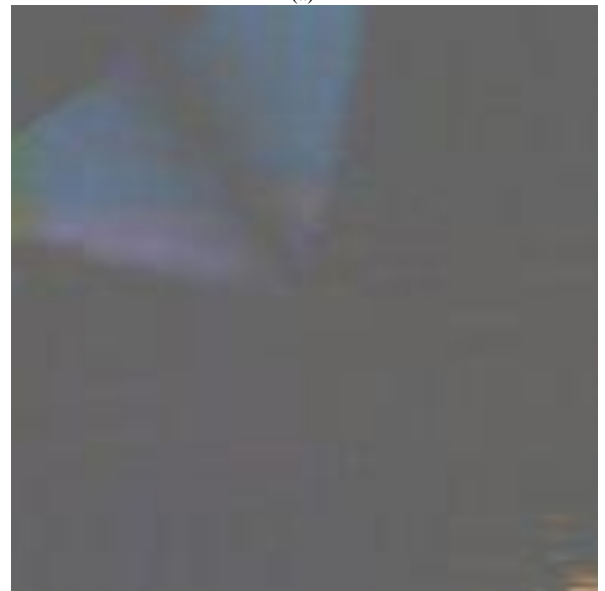


Fig. 9. (a) Color Wheel corrected with Flesh Tone Aperture of  $30^\circ$   
(b) Enhanced Difference on (a) and source



(a)



(b)



(c)

Fig. 10. Oana  
 (a) Oana uncorrected;  
 (b) Oana corrected with Aperture of  $15^0$   
 (c) Oana enhanced differences

The FTC was applied on a synthetic image (a color wheel pattern) and on natural images. The Flesh Tone region is easily visible on the synthetic pattern in Fig.9. (a). Fig.9. (b). shows the color differences between the original and corrected image. Differences are magnified by 2x.

The FTR aperture was narrowed from  $30^0$  as for the synthetic image, to  $15^0$ . The difference map shows that the FTR was extracted correctly – i.e. adjacent colors (pink, yellow) were not affected by the FTC. Only the natural flesh-tone colors have been processed. The difference map in Fig. 10.(c) is a magnified by 10x difference between the original source image (a) and it's corrected version (b)

## V. CONCLUSIONS

The proposed FTC algorithm has significant advantages over similar approaches, resulting in easy programmability of the flesh tone region detection and of the correction strength. The use of a sinusoidal mapping function allows for smooth transitions between non-flesh tone and corrected flesh tone regions. The algorithm is operating only on hue variations, thus the correction to the  $[U V]$  signal is additive. This approach allows for low artefacts and reduced implementation costs.

As a next improvement, the FTC algorithm could be applied directly on graphic images, hence the  $[RGB]$  to  $[YUV]$  followed by the conversion to  $[IQ]$  can be reduced to a simple  $[RGB]$  to  $[IQ]$  matrix transform.

## REFERENCES

- [1] M. Cani-Gascuel and M. Desbrun, "Animation of deformable models using implicit surfaces," *Visualization and Computer Graphics, IEEE Transactions on*, vol. 3, pp. 50, 1997.
- [2] B. D. Mathew, A. Evans, R., "A characterization of visual feature recognition," 2003.
- [3] P. Soo-Chang and T. Ching-Long, "Robust face detection for different chromatic illuminations," 2002.
- [4] Y. Chye Hwang, R. T. Whalen, G. S. Beaupre, S. Y. Yen, and S. Napel, "Reconstruction algorithm for polychromatic CT imaging: application to beam hardening correction," *Medical Imaging, IEEE Transactions on*, vol. 19, pp. 11, 2000.
- [5] Y. Adachi, A. Imai, M. Ozaki, and N. Ishii, "Extraction of face region by using characteristics of color space and detection of face direction through an eigenspace," 2000.
- [6] H. H. S. Ip and C. S. Chan, "Dynamic simulation of human hand motion using an anatomically correct hierarchical approach," 1997.
- [7] J. Keith, *Video Demystified -A Handbook for the Digital Engineer.*, Third Edition ed. ed. Eagle Rock, VA 24085: LLH: Technology Publishing, 1955.
- [8] R. Ekstrand, "A Flesh-Tone Correction Circuit," *Broadcast and Television Receivers, IEEE Transactions on*, vol. BTR-17, pp. 189, 1971.
- [9] C. Engel, G. Tzakis, and G. Srivastava, "A New Chroma Processing Integrated Circuit," *Consumer Electronics, IEEE Transactions on*, vol. CE-25, pp. 577, 1979.
- [10] L. A. Harwood, "A Chrominance Demodulator IC with Dynamic Flesh Correction," *Consumer Electronics, IEEE Transactions on*, vol. 22, pp. 118, 1976.
- [11] P. M. Flamm, "Flesh tone correction circuit." USA.: P. M. Flamm, 1987.
- [12] L. Eung-Joo and H. Yeong-Ho, "Automatic flesh tone reappearance for color enhancement in TV," *Consumer Electronics, IEEE Transactions on*, vol. 43, pp. 1159, 1997.
- [13] L. Eung-Joo and H. Yeong-Ho, "Favorite color correction for reference color," *Consumer Electronics, IEEE Transactions on*, vol. 44, pp. 15, 1998.
- [14] P. M. Flamm, "Flesh Tone Correction Circuit." USA Patent, 1987.